Numerical investigation of bearing capacity of pressed-in piles for earth-based innovations and geotechnical strategies for construction projects on the Moon

H. H. Tamboura
Chief, Scientific Research Section, GIKEN LTD., Kochi, Japan,
Y. Ishihara
Manager, Scientific Research Section, GIKEN LTD., Kochi, Japan
N. Ogawa
Assistant Manager, Scientific Research Section, GIKEN LTD., Tokyo, Japan

ABSTRACT

Construction on the moon faces numerous challenges, including logistical issues, low gravity, unknown lunar subsoil parameters, and more. It is crucial to address these issues before undertaking any construction projects on the moon. The primary objectives of this study are to reproduce the load-settlement curve of any loading test numerically by proposing appropriate joint element parameters and to establish a method for obtaining soil parameters at the site of the loading. The research is built upon the experimental research conducting full-scale field loading tests on Rotary Cutting Pressed-in (RCP) small diameter Piles installed without water injection, a condition anticipated on the Moon. Soil parameters were extracted from Cone Penetration Test (CPT) results near the experimental site, and joint element parameters for numerical analysis were determined using a novel method based on the loading test results. The study employed commercial Finite Element (FE) analysis software to evaluate the vertical and horizontal bearing capacity of both open and closed-ended piles, successfully replicating the loading test results. The agreement with the loading test results underscores the reliability of deriving soil parameters from CPT data and determining joint element parameters through the proposed method. Ultimately, the research contributes a flowchart outlining the back analysis of the Moon's soil parameters from static load tests conducted on the Moon, providing a framework for future lunar geotechnical investigations.

Keywords: *Lunar Construction, Bearing capacity, Tubular pile, Rotary Cutting Press-in, Numerical Analysis*

1. Introduction

In recent years, there has been a growing interest in the potential for lunar exploration and construction projects, which has led to a need for geotechnical engineers to develop suitable foundation designs for these unique environments.

The authors have been participating in the Space Construction Innovation Project (MLIT, 2023) to establish a rational construction process of structures with piles for space, particularly on the Moon (Ishihara et al. 2024). The press-in piling machine can operate in zero-gravity environments since it uses extraction resistance of previously installed piles as a reaction force. One promising solution is the use of small-diameter steel pipe piles, which offer a combination of strength, versatility, and logistical advantages. On Earth, these piles are installed using the 'Rotary Cutting Press-in' (RCP) method (**Fig. 1**) which is adaptive to hard grounds. The authors aim to revolutionize construction worldwide and shape the future of construction on the lunar surface with their innovative RCP technologies (see **Fig.2**).

In the 'press-in' method (International Press-in Association (IPA), 2016), a static jacking force is used to install a pile while a reaction force is obtained from

previously installed piles. In the 'Rotary Cutting Press-in' (RCP method), vertical and rotational jacking forces are applied simultaneously to a pile with teeth on its base. Since the press-in method is a relatively new piling method and is more frequently used for the construction of walls in which the horizontal performance is most important, there has been, until recently, a lack of design methods for the axial capacity of piles installed by this method (Ishihara et al. 2020). Ishihara et al. 2024 have reported the vertical and horizontal capacity of small-diameter steel pipe piles, installed using the RCP method, from static pile load tests along with ground profiles from CPT. The experimental research with full-scale field loading tests is a preliminary and feasibility study of the investigation for press-in pilling on the Moon, hence, this study will be drawing inspiration from this pioneering work of full-scale field loading tests.

Numerical analysis is another powerful tool that allows us to analyze pile behaviors. In numerical analysis, using the right joint elements is crucial to replicating soil-pile interaction under large deformation of soil. MIDAS GTS NX is a software widely used for analyzing complex pile-soil interaction. In this software, it can use the interface wizard interaction to model the stiffness of the pile interface using soil modulus. However, the settings of adequate parameters for the joint elements to reproduce the actual soil-pile interaction have to be determined by the users.

Central to any geotechnical investigation is the understanding of soil parameters. Several methods exist for soil parameter investigation including laboratory testing and field testing like the CPT for real-time measurements of soil resistance. Insights from Robertson and Cabal (2010), Robertson and Campanella (1983), Kulhawy and Mayne (1990), Robertson (2009), and Khitrov et al. (2019) contribute to the understanding of soil properties, correlations, and mechanical relationships. Ishihara et al. (2015a, b) have proposed formulas to obtain equivalent CPT q_c, and equivalent SPT N values of soil from pilling data.

The primary objectives of this research are multifaceted. Firstly, we aim to investigate soil parameters using the CPT data. Subsequently, the study seeks to develop equations for estimating joint elements crucial for numerical analysis in the MIDAS GTX NX software, leveraging the full-scale loading test's load-settlement curves reported by Ishihara et al. (2024). With a focus on bridging theoretical insights and practical applications, the research endeavors to reproduce the load-settlement curves of the full-scale loading tests using the proposed joint elements equations within the software's standard framework. The ultimate goal of this study is to propose a comprehensive flow chart that outlines the process of obtaining lunar soil parameters from pile load test results on the moon.

(a) Typical press-in piling machine for tubular pile

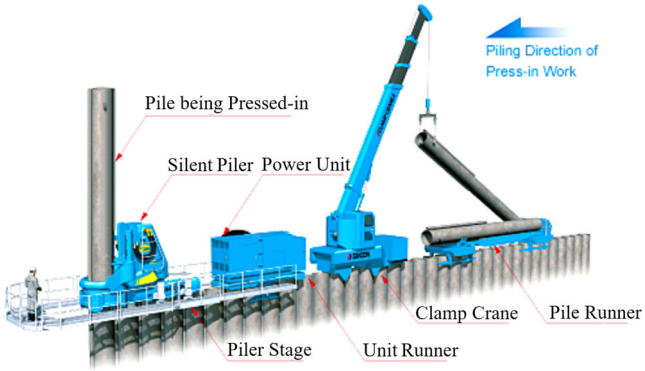

(b) GRB System™ (GIKEN Reaction Base System)

Fig. 1 Typical press-in pilling method for tubular piles

Fig. 2 Illustration of Press-in piling on the Moon

2. Background and objectives of this study

In the press-in method, the piling data (information obtained during piling, such as press-in force and torque) can be obtained for all the piles (Ishihara et al., 2024). If the press-in piling method is applied to construction projects on the Moon, it could facilitate a rational construction process even though information from preliminary investigations is limited. According to Ishihara et al. (2024), the process of using the press-in method and associated data on the Moon is illustrated in **Fig. 3**. Specifically, as shown in the left-hand side cycle of **Fig. 3**, the main process could be as follows: (1) the "design" of structures is roughly implemented based on the limited information in the "investigation", (2) the piling work is conducted in "construction work" while yielding the estimated subsurface information and pile capacity, (3) the information in "investigation" is supplemented by the estimated information obtained in "construction work", and the content of "design" is validated and updated based on the estimated information in "construction work". In addition, as shown in the right-hand side cycle of **Fig. 3**, the press-in machine used for the construction process in the left-hand side cycle of the figure could also be applied to conducting a static loading test (simplified loading test) (step II), to obtain information on the performance of the pressed-in piles on the Moon. The results from this simplified loading test could then be used in numerical analysis ("Analysis") to investigate lunar subsurface conditions and refine the design method (Step III). The information from the "investigation" is further supplemented by the data obtained in the "Analysis" (Step IV), and the design is validated and updated based on these findings (Step IV).

The main objective of this study is to propose an investigation model that follows the steps outlined in the right-hand cycle of **Fig. 3** based on the field experiment conducted by Ishihara et al. (2024).

The field study by Ishihara et al. (2024) involved full-scale loading tests on small-diameter steel tubular piles, utilizing the rotary cutting piling method. CPT tests were concurrently conducted for soil investigation, and two types of piles, closed-end and open-end, were employed, each having an outer diameter of 318.5 mm and an embedment length of 4.1m. Vertical loads were applied at the pile head, with horizontal loading near the ground level.

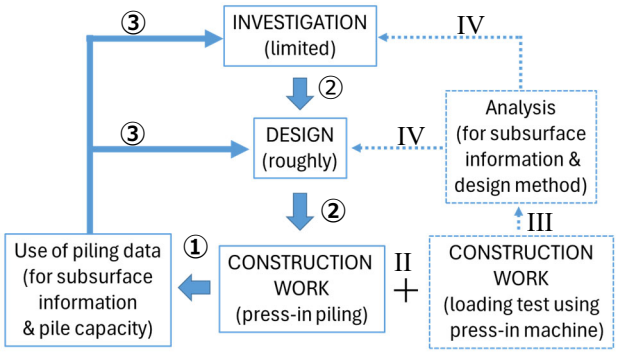

Fig. 3 Construction Process on the Moon (After Ishihara et al., 2024)

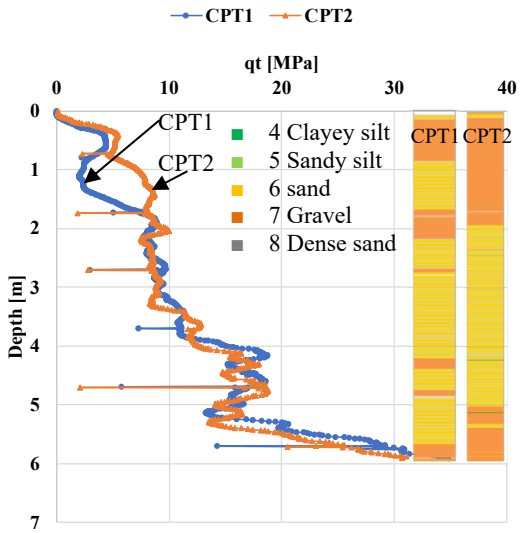

(a) Cone resistance

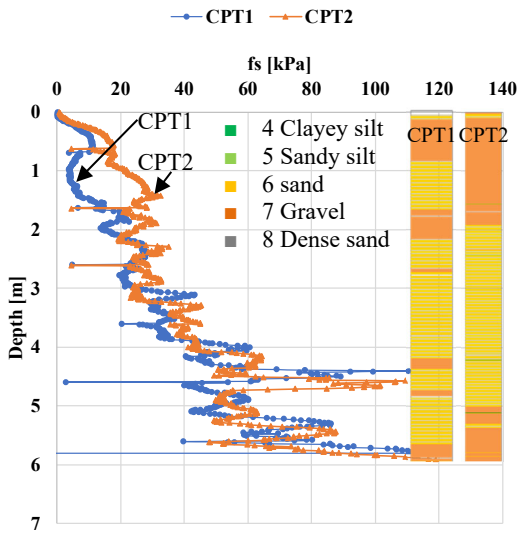

(b) Cone sleeve friction

Fig. 4 CPT test results (after Ishihara et al. 2024)

The CPT results along with the ground geological

cross-section and loading test outcomes are illustrated in **Figs. 3** and **4**, respectively. These served as inputs for estimating soil parameters and validating the numerical method in this study. Notably, the open-end pile demonstrated higher vertical capacity, while the closed-end pile exhibited slightly superior horizontal capacity.

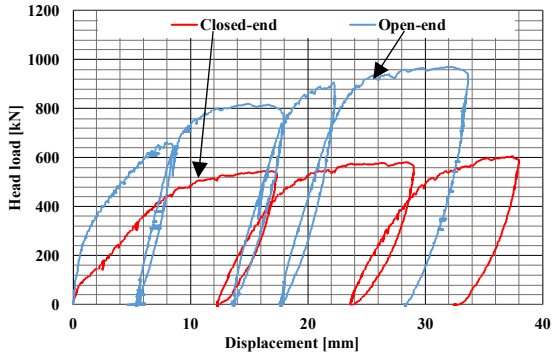

(a) Vertical loading tests

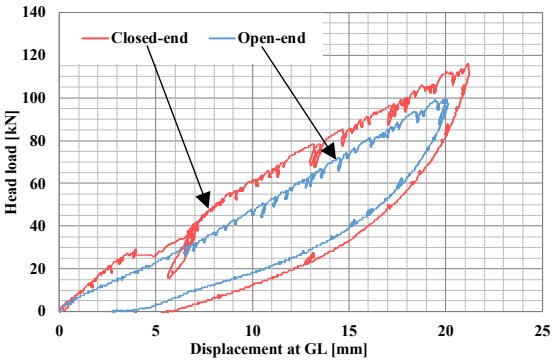

(b) Horizontal loading tests

Fig. 5 Load-displacement curves (after Ishihara et al. 2024)

3. Investigation of soil parameter

Robertson and Cabal (2010) delved into the estimation of soil unit weight using CPT results and put forth a formula for unit weight calculation. The relationship, as proposed by Robertson (2010), articulates the soil unit weight in relation to the friction ratio and cone resistance, formulated as **Eq. (1)**. This formula provides a means to derive an estimate of soil unit weight based on the results through CPT in this study.

$$\gamma/\gamma_w = 0.27(\log R_f) + 0.36\left[\log\left(\frac{q_t}{P_a}\right)\right] + 1.236 \qquad (1)$$

where R_f is the friction ratio, γ_w is the unit weight of water, q_t is the corrected cone resistance, and P_a is the atmospheric pressure.

Several correlations exist between friction angle (ϕ') and CPT parameters. Robertson and Campanella (1983) introduced a correlation for estimating the peak friction angle in sands. Another relationship for sands was suggested by Kulhawy and Mayne (1990), and is expressed in **Eq. (2)** below.

$$\phi' = 17.6 + 11 \log Q_{tn} \qquad (2)$$

Where Q_{tn} is the normalized cone resistance.

Robertson (2009) investigated the relationship between soil Young's modulus and CPT results. According to their findings, the soil Young's modulus can be estimated using **Eq. (3)** below.

$$E = \alpha_E(q_t - \sigma_{vo}) \qquad (3)$$

Where q_t is the corrected cone resistance and σ_{vo} is the vertical total stress. The coefficient α_E can be obtained from **Eq. (4)** below.

$$\alpha_E = 0.015[10^{0.55I_c+1.68}] \qquad (4)$$

Where I_c is the Soil Behavior Type Index.

Khitrov et al. (2019) investigated the interrelations of mechanical properties in various soil types. They demonstrated the connection between the mechanical parameters frictional angle $\phi[°]$ and cohesion $c\,[kPa]$ with Young's modulus E [MPa] through power dependencies, as expressed in **Eq. (5)** and **Eq. (6)**.

$$\phi = A_{\varphi E}E^{B_{\varphi E}} \qquad (5)$$

$$c = A_{CE}E^{B_{CE}} \qquad (6)$$

where $A_{\varphi E}$, $B_{\varphi E}$, A_{CE}, and B_{CE}, are numerical coefficients. For coarse sand $A_{\varphi E} = 15.49$, $B_{\varphi E} = 0.26$, $A_{CE} = 0.0005$ and $B_{CE} = 2.16$.

Using the aforementioned equations, the soil parameters. for the field test location were determined and illustrated in **Fig. 6**. Based on the results, a soil unit weight of 18 kN/m³ and an internal frictional angle of 40° were adopted. Cohesion and Young's modulus were estimated

to exhibit linear increases with depth, as shown in **Fig. 6(b)(d)**. These functions can be directly incorporated into MIDAS GTS NX.

Fig. 6(c) allows for a comparison of **Eq. (5)** and **Eq. 2**. The discrepancy observed is due to the dependency on Young's modulus (E) in **Fig. 6b** of the internal friction angle ϕ determined from **Eq. (5)**. However, the average values remain almost the same.

interaction. In this study, MIDAS GTS NX serves as the numerical analysis tool.

The model geometry and mesh used are presented in **Fig. 7**. The pile has an outer diameter of 318.5 mm and is embedded 4.1 m in the ground; these dimensions reflect those of the pile used in the field tests. To minimize boundary effects, the domain extends approximately 20 times the pile diameter (D) in horizontal dimensions, and

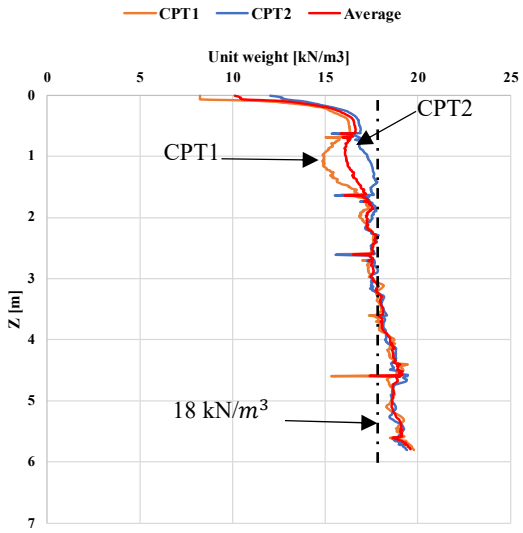

(a) Unit weight

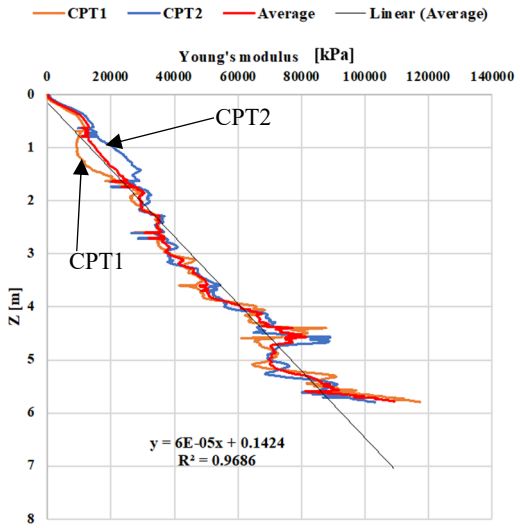

(b) Young's modulus

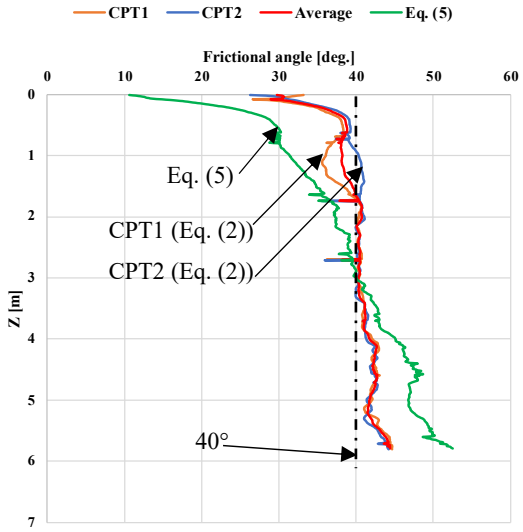

(c) Internal friction angle

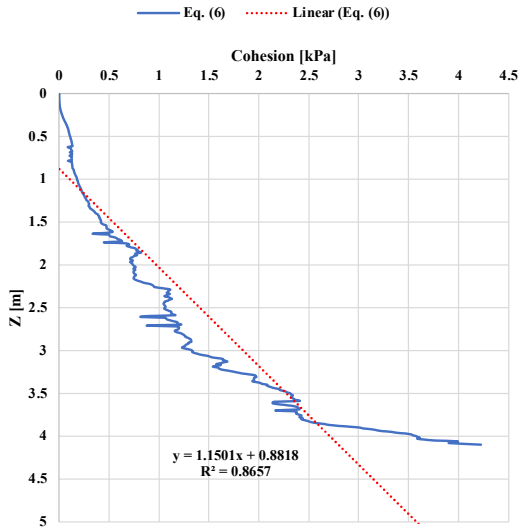

(d) Cohesion

Fig. 6 Calculated soil parameter from CPT data obtained on the field test

4. Numerical model

MIDAS GTS NX is a finite element analysis software used by geotechnical engineers for the analysis of soil and rock deformation, stability, and soil-structure

the pile tip is about 20 times D from the bottom of the domain (D = Pile diameter). The software's automatic setting detects outer boundaries and configures boundary conditions accordingly. The model's bottom is fixed,

restricting movements in all directions. Finer meshes around the pile capture higher deformations. Joint elements were adopted at the pile-soil interface to mediate interactions between the pile and the ground.

Two types of loads were applied: vertical and horizontal. For vertical loading, the load increased from 0 kN to 1000 kN in 100 kN increments at the pile head. For horizontal loading, three conditions were considered with different loading heights (h): ground level, which corresponds to the experimental condition, (h=0m); 0.5 m above the ground (h=0.5m); and 1 m above the ground (h=1m). The load increased from 0 kN to 200 kN with a 20 kN increment.

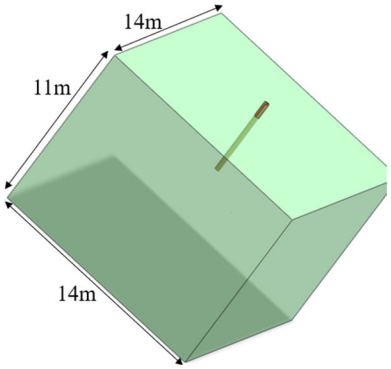

(a) Perspective view of the geometry

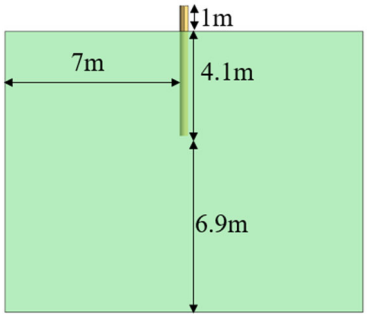

(b) Side view of the geometry

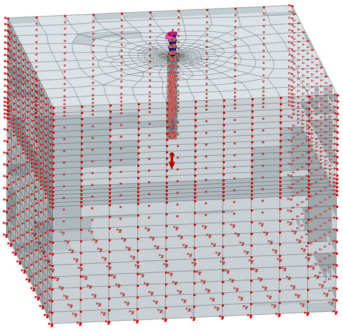

(c) Mesh and boundary conditions

Fig. 7 Geometry, mesh, and boundary conditions

Numerical analysis considered soil parameters from **Fig. 6** and pile geometries adopted in the experiment (**Section 2**). Pile properties included Young's modulus of 205.10^6 kN/m^2, unit weight of 78.5 kN/m^3, and Poisson's ratio of 0.28. The pile is made of steel material.

5. Proposal of identifying joint elements parameters based on load test results

The joint element parameters are crucial in numerical simulations using MIDAS, especially when employing the "Pile" joint element type, where five parameters are essential: "Tip Bearing Capacity," "Tip Spring Stiffness," "Ultimate Shear Force," "Shear Stiffness Modulus," and "Normal Stiffness Modulus."

This study proposes a method to determine the joint element parameters based on the load-settlement curve obtained from field tests. **Fig. 8** illustrates a typical curve with an Initial Linear Region, a Transitional Region, and a Final Linear Region. The following parameters are needed for the pile tip: "Tip Bearing Capacity" and "Tip Spring Stiffness." The "Tip Bearing Capacity" is taken as the capacity when the settlement is 10% of the pile diameter (δ_{L2}), denoted as Q_{L2} in **Fig. 8**. The study found that the "Tip Spring Stiffness" parameter influences the slope of the curve's Final Linear Region. Then "Tip Spring Stiffness" shall be defined as the slope of the tangent line at (δ_{L2}, Q_{L2}), as expressed by **Eq. (7)** below.

$$Tip\ Spring\ Stiffness = \frac{dQ}{d\delta}(\delta_{L2})\ [kN/m] \qquad (7)$$

Parameters Q_{L2}, δ_{L2} are defined in **Fig. 8**. For the pile shaft, three parameters are required: "Ultimate Shear Force," "Shear Stiffness Modulus" (Kt), and "Normal Stiffness Modulus" (Kn). It could be interpreted that the Initial Linear Region of a load-settlement curve (refer to **Fig. 8**) primarily results from the pile's shaft friction, while the Transitional Region marks the beginning of the pile tip's large contribution. This study proposes that the "Ultimate Shear force" is the frictional stress defined at the midpoint (δ_S, Qs) of the Transitional Region of the curve, as expressed by **Eq. (8).**

$$Ultimate\ Shear\ Force = \frac{Q_S}{A_S}\ [kN/m^2] \quad (8)$$

Where A_s is the pile shaft area. The "Shear Stiffness Modulus" (K_t) parameter is observed to impact the curvature of the Transitional Region of the curve. To consider this, K_t shall be taken as the slope of the tangent line at (δ_S, Qs) and **Eq. (9)** is proposed to estimate it.

$$K_t = \left[\frac{dQ}{d\delta}(\delta_S)/A_S\right] \times a\ [kN/m^3] \quad (9)$$

The "Normal Stiffness Modulus" (K_n) parameter may be associated with the slope of the Initial Linear Region of the curve and shall be determined using **Eq. (10)** below.

$$K_n = \left[\frac{dQ}{d\delta}(\delta_{L1})/A_S\right] \times a\ [kN/m^3] \quad (10)$$

Note that for the simulation of horizontal capacity, the pile tip parameters are not necessary. The letter "*a*" in **Eq. (9)** and **Eq. (10)** is a factor that is supposed to represent a factor related to the pile material. Since "a" serves as a coefficient associated with the pile material, it remains constant regardless of the values of Q_S, and Q_{L1}, provided that the pile material remains unchanged. Therefore, the same value of "a" should be applied in both **Eq. (9)** and **Eq. (10)**. The value of "a" for carbon steel material will be discussed in the following section.

Note that the determination of Q_S, Q_{L1}, δ_S, and δ_{L1} requires engineering judgment.

Using the above-explained method, joint element parameters were determined based on the load settlement curve in **Fig. 5**. The parameters are presented in **Table 1**.

The relationship between K_n and K_t may be assumed as $K_t = K_n \times K \times \tan\delta$, where K and δ are the coefficient of earth pressure and the friction angle at the pile-soil interface. Considering the typical ranges of K (0.5 - 3) and δ (20 – 30 degrees), the value of $K \times \tan\delta$ ($=K_t/K_n$) ranges between 0.6 and 5.6. This range corresponds to the values you obtained (in **Table 1**).

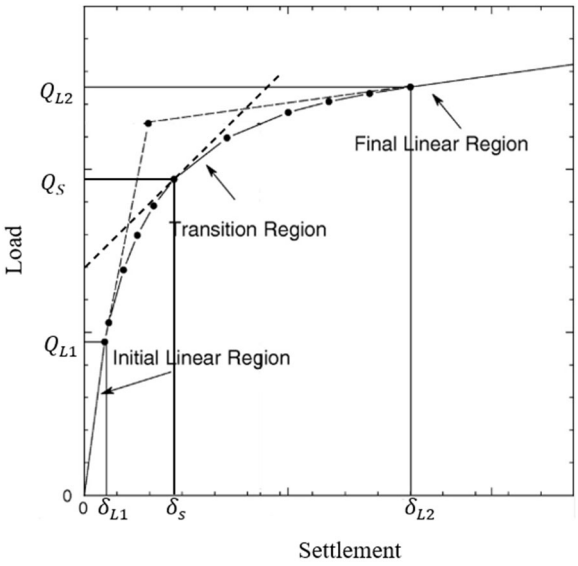

Fig. 8 Joint element investigation method

6. Comparison of numerical results and field test results (validation of the numerical model)

The estimated joint element parameters were utilized in MIDAS GTS NX to assess the pile capacity using the Mohr-Coulomb model, obtaining both vertical and horizontal capacities for closed-end and open-end piles. The comparison between numerical and field test results is illustrated in **Fig. 9**. Numerical analysis was performed for various values of "a". The results in **Fig. 9** reveal a satisfactory alignment between numerical and field test outcomes when "a" equals 20. The proposed joint element parameters exhibit better fitting of the loading test results than the joint elements from MIDAS' manual. These findings affirm that the proposed numerical model and calculated joint elements can effectively replicate full-scale loading test results, indicating its applicability to

Table 1 calculated joint element parameters

	For Pile Tip		For Pile Shaft		
	Tip Bearing Capacity (kN)	Tip Spring Stiffness (kN/m)	Ultimate Shear Force (kN/m^2)	Shear Stiffness Modulus (kN/m^3)	Normal Stiffness Modulus (kN/m^3)
Closed End Pile	580	2652.17	106.53	12428.41a	35313.01a
Open End Pile	970	11500	146.79	17886.18a	78048.78a

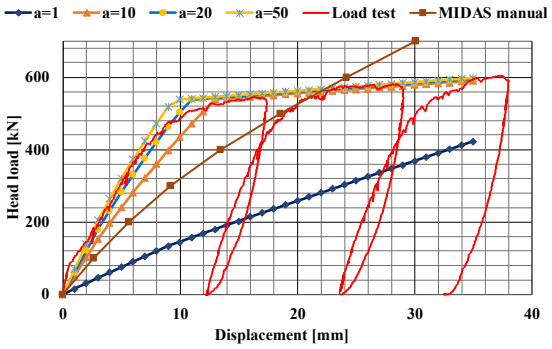

(a) Vertical capacity of closed-end pile

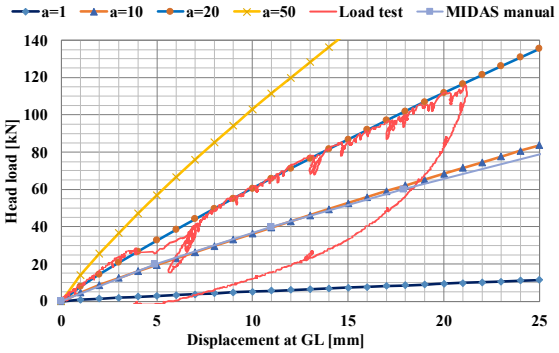

(b) Horizontal capacity of closed-end pile

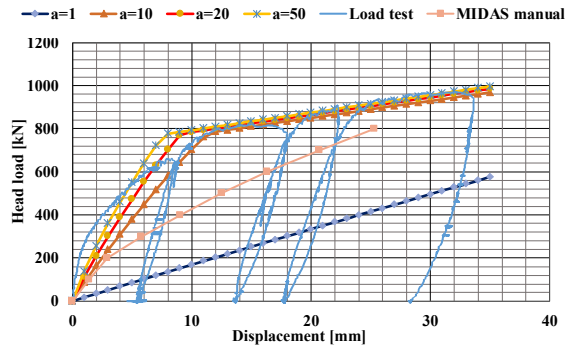

(c) Vertical capacity of open-end pile

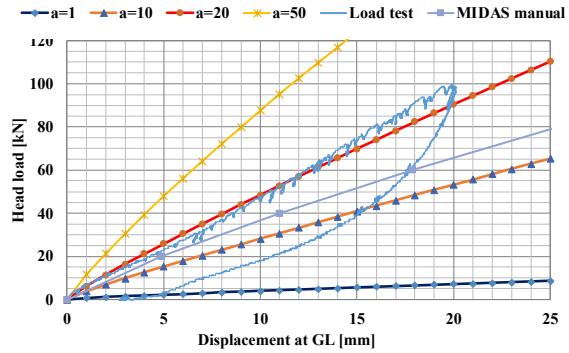

(d) Horizontal capacity of open-end pile

Fig. 9 Validation of the numerical model

piling on the Moon using loading test method. An intriguing observation is the surprisingly higher vertical bearing capacity of the open-end pile. This phenomenon could be attributed to pile plugging, which generates friction on the inner side of the pile. As reported by Ishihara et al. (2024), the inner soil length of the open-end pile was approximately 1.5 m. This indicates that, for small-diameter piles, an open-end configuration might exhibit higher capacity than a closed-end pile. However, further investigations are warranted to provide clarity on this phenomenon; the objective of this study being the reproduction of experimental results.

The impact of loading height (h) on horizontal capacity was also explored in the numerical analysis. Horizontal capacities for h = 0, 0.5, and 1m are depicted in **Fig. 10**. The results demonstrate that an increase in loading height leads to a reduction in horizontal capacity for both closed-end and open-end piles. Specifically, the capacity loss is estimated at 46.57% for the closed-end pile and 32.52% for the open-end pile.

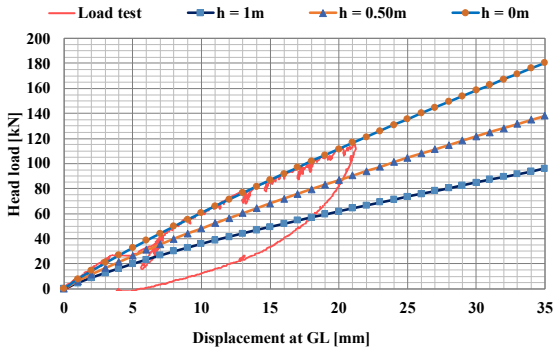

(a) Horizontal capacity of closed-end pile

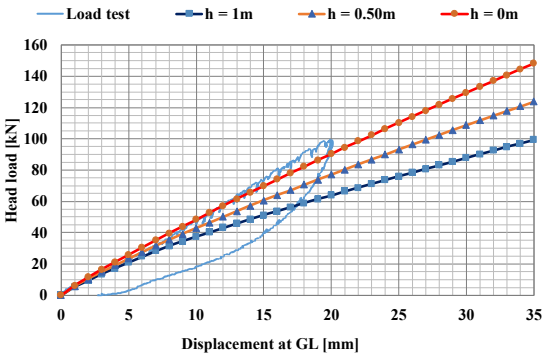

(b) Horizontal capacity of open-end pile

Fig. 10 Effect of loading height on the horizontal capacity

7. Back Analysis of soil parameters

Bowles (1977) has established a relationship between unit weight (γ) [kN/m^3] and the corresponding friction angle ϕ[°] for sand, as per **Table 2** (Das et al. 2019).

This study has successfully established a relationship between the load-settlement curve and joint element parameters. Leveraging this relationship, a back analysis method for obtaining soil parameters is proposed, involving the following steps:

1. Obtain Load-Settlement Curve: Acquire a load-settlement curve from the loading test (Ex: load-settlement curve from the loading test on the Moon).

2. Calculate Joint Element Parameters: Use the established relationship in this study and the load-settlement curve to compute joint element parameters.

3. Choose a Young's Modulus: Select a reasonable value (or function) for Young's modulus of soil and calculate the corresponding internal frictional angle and cohesion using **Eq. (5)** and **Eq. (6).** The unit weight is then obtained using the calculated frictional angle in **Table 2**.

4. Perform Numerical Analysis: Utilize the obtained soil parameters from **step (3)** and the calculated joint elements from **step (2)** to conduct numerical analysis in MIDAS, resulting in a load-settlement curve.

5. Compare Curves: Compare the load-settlement curves obtained from the loading test and analysis.

6. Iterate: Repeat the process from **step (3)** by changing the Young's modulus of soil until achieving a satisfactory match between the two load-settlement curves.

The effectiveness of this method is demonstrated in **Fig. 11**, where a comparison of the load-settlement curve from the loading test and the numerical analysis is presented. The influence of varying Young's modulus is evident. Based on the results in **Fig. 11**, it is concluded that the method can provide reasonable values for soil parameters with a confidence level of at least 80%.

This study has introduced a method to obtain lunar soil parameters. The proposed approach combines the simplified loading test using the press-in machine with numerical analysis using MIDAS GTS NX, as outlined in the flow chart in **Fig. 12**. The key steps include conducting loading tests in lunar simulant conditions, obtaining soil parameters through field/lab experiments, estimating joint element parameters, performing numerical analysis, and back-analyzing soil parameters.

Table 2. Unit weights and the associated friction angles for sand, after (Bowles 1977); used by (Das et al. 2019).

φ	30	32	34	36	38	40	42	44
γ	13.5	14.5	15	16	16.5	17.5	18	19

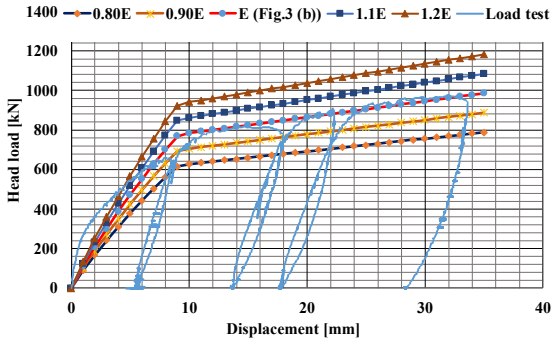

(a) Based on the vertical capacity of the open-end pile

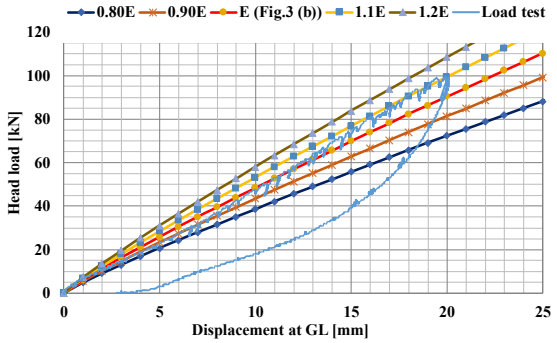

(b) Based on the horizontal capacity of the open-end pile

Fig. 11 Back analysis of soil parameters

8. Conclusion

This paper presented a novel framework for geotechnical engineering analysis, specifically focusing on the estimation of joint element parameters for numerical simulations. The developed equations, derived from full-scale loading test results, successfully reproduced load-settlement curves within the MIDAS GTS NX software.

Furthermore, the study introduced a comprehensive flow chart that outlines a systematic approach to extract crucial lunar soil parameters using load test results on the Moon. By combining a simplified loading test conducted by the press-in machine and numerical analysis, this method provides an avenue for obtaining insights into the geotechnical properties of lunar environments.

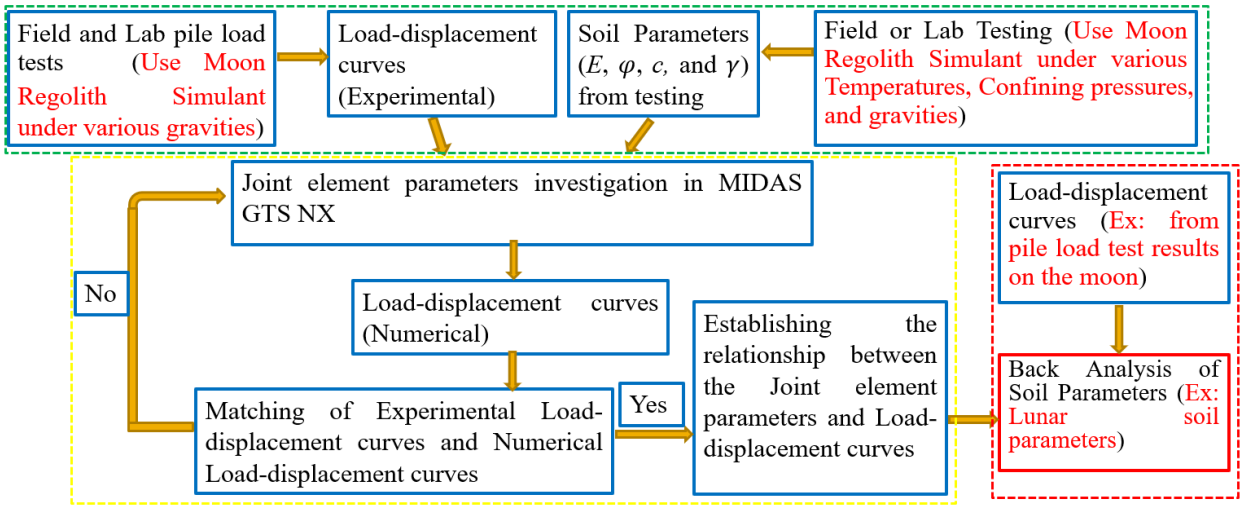

Fig. 12. Flow chart for soil parameters investigation based on loading test results

9. Acknowledgment

This research was conducted as part of the "Space Construction Innovation Project" of the Ministry of Land, Infrastructure, Transport and Tourism in Japan. The authors would like to express their gratitude to all those involved.

References

Bowles, J.E., 1977. Foundation analysis and design. New York: McGraw- Hill.

Das P. P., Khatri V. N., and Dutta R. K., Bearing capacity of ring footing on weak sand layer overlying a dense sand deposit. Geomechanics and Geoengineering, Vol. 16, Issue 4, 2019, pp. 249-262.DOI: 10.1080/17486025.2019.1664775.

International Press-in Association (IPA), 2016. Press-in retaining structures: a handbook, First edition 2016, pp. 4.23-4.24.

Ishihara, Y., Haigh, S., Koseki, J., 2020. Assessment of base capacity of open-ended tubular piles installed by the Rotary Cutting Press-in method. Soils and Foundations, Volume 60, Issue 5, PP. 1189-1201.

Ishihara, Y., Haigh, S. and Bolton, M. D. 2015. Estimating base resistance and N value in rotary press-in. Soils and Foundations, Vol. 55, No. 4, pp. 788-797.

Ishihara, Y., Ogawa, N., Okada, K. and Kitamura, A. 2015. Estimating subsurface information from data in pressin piling. Proceedings of the 5th International Workshop in Ho Chi Minh, Press-in Engineering 2015, pp. 53-67.

Ishihara, Y., Eguchi, M., Mori, A., Toda, Y., 2024. Use of press-in pilling data for construction on the Moon: estimating subsurface information and pile capacity. Proceedings of 3rd International Conference on Press-in Engineering 2024, Singapore.

Khitrov, E.G., Andronov A.V., Martynov B.G., Spiridonov S.V., 2019. Interrelations of various soil types mechanical properties. Journal of Physics: Conf. Series 1177 (2019) 012032.

Kulhawy, F.H., and Mayne, P.H., 1990. Manual on estimating soil properties for foundation design, Report EL-6800 Electric Power Research Institute, EPRI, August 1990.

Robertson, P. K., 2009. Interpretation of cone penetration tests–a unified approach. Canadian Geotech. J.,46(11), PP. 1337–1355.

Robertson, P.K., and Cabal, K.L., 2010. Estimating soil unit weight from CPT. 2nd International Symposium on Cone Penetration Testing, Huntington Beach, CA, USA, May 2010.

Robertson, P.K., and Campanella, R.G., 1983a. Interpretation of cone penetration tests – Part I (sand). Canadian Geotechnical Journal, 20(4):718-733.

Robertson, P.K., and Campanella, R.G. 1983b. Interpretation of cone penetration tests – Part II (clay). Canadian Geotechnical Journal, 20(4): 734-745.